Journal of Medicinal Chemistry

Article

pubs.acs.org/jmc

Structure–Activity Relationships of Chromone Derivatives toward the Mechanism of Interaction with and Inhibition of Breast Cancer Resistance Protein ABCG2

Evelyn Winter,[†,‡,▽] Florine Lecerf-Schmidt,[§,▽] Gustavo Gozzi,[†,∥] Basile Peres,[§] Mark Lightbody,[§] Charlotte Gauthier,[†] Csilla Ozvegy-Laczka,[⊥] Gergely Szakacs,[⊥] Balazs Sarkadi,[#] Tânia B. Creczynski-Pasa,[‡] Ahcène Boumendjel,[§,○] and Attilio Di Pietro*[,†,○]

[†]Equipe Labellisée Ligue 2013, BMSSI UMR 5086 CNRS/Université Lyon 1, IBCP, 69367 Lyon, France

[‡]Department of Pharmaceutical Sciences, PGFAR, Federal University of Santa Catarina, Florianopolis, Santa Catarina, Brazil

[§]Département de Pharmacochimie Moléculaire, UMR5063 CNRS-Université Joseph Fourier de Grenoble I, Grenoble, France

[∥]Department of Biochemistry and Molecular Biology, Federal University of Parana, Curitiba, Paraná, Brazil

[⊥]Institute of Enzymology, Center for Natural Sciences, Hungarian Academy of Sciences, Budapest, Hungary

[#]Molecular Biophysics Research Group, Hungarian Academy of Sciences, Semmelweiss University, Budapest, Hungary

ABSTRACT: We recently identified a chromone derivative, 5-(4-bromobenzyloxy)-2-(2-(5-methoxyindolyl)ethyl-1-carbonyl)-4*H*-chromen-4-one, named here as chromone **1**, as a potent, selective, nontoxic, and nontransported inhibitor of ABCG2-mediated drug efflux (Valdameri et al. *J. Med. Chem.* **2012**, *55*, 966). We have now synthesized a series of 14 derivatives to study the structure–activity relationships controlling both drug efflux and ATPase activity of ABCG2 and to elucidate their molecular mechanism of interaction and inhibition. It was found that the 4-bromobenzyloxy substituent at position 5 and the methoxyindole are important for both inhibition of mitoxantrone efflux and inhibition of basal ATPase activity. Quite interestingly, methylation of the central amide nitrogen strongly altered the high affinity for ABCG2 and the complete inhibition of mitoxantrone efflux and coupled ATPase activity. These results allowed the identification of a critical central inhibitory moiety of chromones that has never been investigated previously in any series of inhibitors.

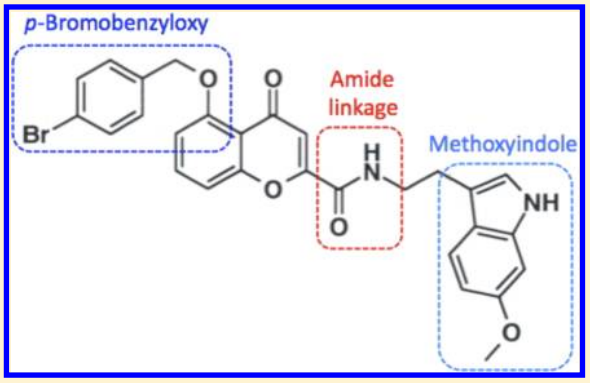

INTRODUCTION

Anticancer chemotherapy is hampered by cross-resistance of tumor cells to cytotoxic drugs. The involved mechanisms are diverse and often lead to an intracellular decrease of the anticancer drugs. One of these mechanisms is attributed to transmembrane efflux pumps belonging to the large family of ATP-binding cassette (ABC) proteins that use ATP hydrolysis as a source of energy to catalyze the efflux of a large panel of cytotoxic agents. Among these ABC transporters, three are now well-recognized to play a key role in the efflux of chemotherapeutics from cancer cells: P-glycoprotein (P-gp, ABCB1),[1] multidrug resistance protein 1 (MRP1, ABCC1),[2] and breast cancer resistance protein (BCRP, ABCG2).[3−5] One of the strategies to abolish tumor resistance to chemotherapy is to develop selective and nontoxic inhibitors of P-gp, MRP1, and BCRP. The combination of inhibitors with anticancer drugs should lead to higher accumulation of the drug inside the cell, allowing for the efficient antiproliferative action of the anticancer drugs.

BCRP/ABCG2, the most recently discovered of the three multidrug transporters, was described to act as a half-transporter requiring at least dimerization to be functional, whereas P-gp and MRP1 act as full-transporters. ABCG2 was reported to confer resistance to a panel of structurally unrelated chemotherapeutic drugs, constituting a major hurdle to chemotherapy success. Intense investigations were therefore aimed at developing ABCG2 inhibitors to be used as reversal agents in combination with anticancer drugs. Recently, a panel of highly active and selective inhibitors was reported for which the activity was ascertained by both accumulation assays and cytotoxicity when combining inhibitors with anticancer drugs.

The first selective inhibitor of ABCG2 was fumitremorgin C (FTC),[6] which, because of its high neurotoxicity, was found to be clinically useless. Synthetic analogues, such as Ko143, were then conceived and allowed the identification of less toxic and more potent inhibitors.[7,8] The P-gp inhibitors tariquidar and elacridar were used as templates for designing new and potent ABCG2 inhibitors;[9−12] however, no mechanistic data are available regarding the inhibitory effects.

Received: July 11, 2013
Published: December 4, 2013

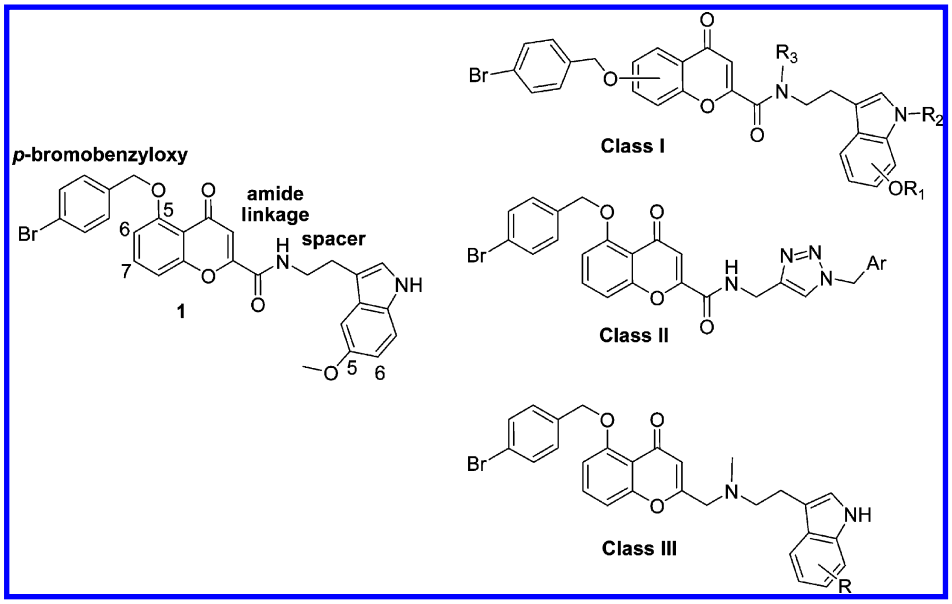

Figure 1. Sites of modifications on the previously identified ABCG2 inhibitor chromone **6g**/MBLII-141, renamed here as chromone **1**.

Scheme 1[a]

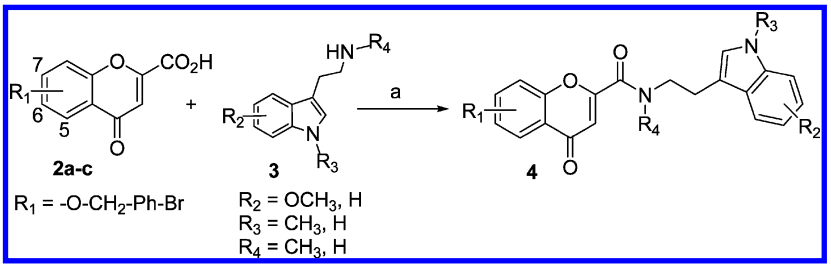

[a]Reagents and conditions: EDC, HOBt, Et_3N, DMF, rt.

Very recently, we reported that chromones bearing a tryptamine moiety were potent, highly selective, and nontoxic inhibitors of ABCG2. We identified three key structural features contributing to the inhibition activity: the presence of a *p*-bromobenzyloxy group at the A-ring of chromone, the chromone moiety, and a tryptamine unit linked to chromone via an amide linkage.[13,14] Hence, chromone **1** (Figure 1) was ranked among the most promising inhibitors of ABCG2 ever reported. To understand better the structure−activity relationships and their influence on the mechanism of interaction with ABCG2, we investigated new derivatives of chromone **1** by emphasizing three classes of analogues (Figure 1). The *p*-bromobenzyloxy substituent was moved among positions 5, 6, or 7 of the chromone ring in class I, the central linker separating the chromone and indolic rings was modified in class II, and the amide linkage was reduced to an amine in class III. In addition, the influence of N methylation of the amide functional group and of the indolic ring was studied within class I to evaluate the donor−acceptor behavior of the NH bond. Furthermore, the differential effects produced on ATPase activity were analyzed.

CHEMISTRY

The access to class I derivatives is shown in Scheme 1. Substituted chromone carboxylic acids **2a−c** were prepared according to our previously reported method[13,15] with a shorter reaction time (3 h instead of 10 h). Carboxylic acids **2a−c** were stepped into a peptide-coupling reaction with tryptamine analogues (**3**) using hydroxybenzotriazole (HOBt) and 1-ethyl-3-(3-dimethylaminopropyl)carbodiimide (EDC) as coupling agents in DMF in the presence of triethylamine (Et_3N) to provide final compounds (**4**) with 11−45% yields.[16] Tryptamine analogues were either commercial (for 5- and 6-methoxytryptamine) or synthesized (for N methylated tryptamine) according to known procedures.[17,18] For methylation of the primary amine of tryptamine, the methyl group was introduced via an ethyl carbamate followed by a reduction with lithium aluminum hydride.[19] N methylation at the indolic ring was carried out by starting from *N*-Boc tryptamine with methyl iodide in the presence of sodium hydroxide and tetrabutylammonium hydrogen sulfate and then removing the Boc group with trifluoroacetic acid.[20]

The synthesis of derivatives belonging to class II is shown in Scheme 2. In this series, we maintained the *p*-bromobenzyloxy at C-5 of chromone. Hence, carboxylic **2a** was reacted with propargylamine under peptide-coupling conditions (HOBt and EDC in DMF in the presence of Et_3N) to afford amide (**5**) with 44% yield. Thereafter, the obtained propargylamide (**5**) was taken on Huisgen reaction with the corresponding arylmethylen azide (**6**) in DMF at room temperature. The 1,3-dipolar cycloaddition was catalyzed by copper sulfate and sodium ascorbate and gave only one isomer for the triazolic compounds (**7**) with 10−46% yields.[21,22] The azide derivatives used in the later reaction were either purchased (benzylazide and 4-bromobenzylazide) or synthesized (3-indolylethan-1-azide)

dx.doi.org/10.1021/jm401649j | J. Med. Chem. 2013, 56, 9849−9860

Scheme 2[a]

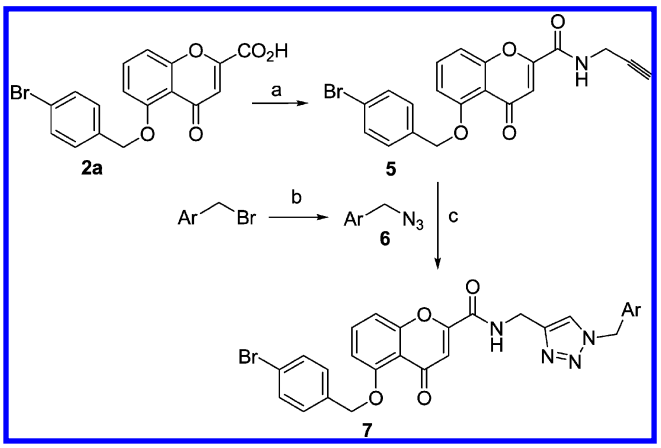

[a]Reagents and conditions: (a) propargylamine, EDC, HOBt, Et_3N, DMF, rt; (b) NaN_3, DMF, rt; (c) $CuSO_4 \cdot 5H_2O$, sodium ascorbate, DMF, rt.

by reaction of sodium azide with 1-bromo-3-indolylethan by nucleophilic substitution performed at room temperature in DMF.

The class III compounds were obtained by reduction of the amide junction according to Scheme 3. Hence, the ester of chromone carboxylic acid **2a**[23] was reduced by sodium borohydride in methanol to provide the corresponding alcohol (**8**) with 26% yield. The latter compound was transformed to the tosylate derivative (**9**) by means of *p*-toluensulfonyl chloride and Et_3N in CH_2Cl_2 at 20 °C. Finally, the tosylate (**9**) was reacted with tryptamine derivatives in DMF without any base to avoid potential indolic N alkylation, providing analogues **10** with 31−38% yield.

BIOLOGICAL EVALUATION

Inhibition of ABCG2-Mediated Drug Efflux. The 14 newly synthesized chromone derivatives were analyzed, together with chromone **1** (Figure 1) as a reference, for their ability to inhibit mitoxantrone efflux and increase its accumulation in ABCG2-transfected HEK293 cells relative to ABCG2-negative control cells. Table 1 (left half) and Figure 2 show that **4a**, only differing from chromone **1** by the methoxy group being located at position 6 of the indolyl ring instead of position 5, displayed the same potent inhibition as chromone **1** on transfected cells, with an EC_{50} of 0.10 μM and a complete maximal inhibition, in a similar way as reference inhibitor Ko143. As expected, the *p*-bromobenzyloxy substituent at position 5 was important for high-affinity inhibition, as its shift to vicinal positions 6 and 7, in **4f** and **4i**, respectively, produced 3- (0.29 μM) and 13-fold (1.27 μM) increases in EC_{50} versus **4a**. The role of the indole moiety was also confirmed because changing its position through insertion of a triazole spacer in **7c** produced a 5-fold loss in affinity (EC_{50} = 0.49 μM), and its replacement by phenyl in **7a** produced a strong additional alteration (1.52 μM), whereas an intermediate effect was observed with bromo-phenyl in **7b** (0.57 μM).

The most original and unexpected effects were obtained upon modification of the central amide linkage: a simple N methylation in **4e** and **4c** produced a 9−11-fold alteration, with respective EC_{50} values of 0.96 and 1.11 μM. Such an effect appeared additive to that produced upon shifting *p*-bromobenzyloxy to position 6 because a 21−26-fold alteration was observed in **4h** and **4g**, with respective EC_{50} values of 2.06 and 2.58 μM and the maximal inhibition being limited to 50−54%. An additional negative effect was obtained upon the introduction of a positive charge to the methylated nitrogen in **10a**, with a strong cumulated alteration (EC_{50} = 1.77 μM and a maximal inhibition limited to 46%) when compared to **10b** for taking into account the small effect (25% decrease in maximal inhibition) produced by peptidic carbonyle deletion. Another small effect was produced upon methylation of the indole nitrogen in **4b** (EC_{50} = 0.30 μM) versus **4a** and chromone **1** (0.10−0.13 μM), which was not additive to the stronger effect produced by methylation of the amide nitrogen in **4d** (1.00 μM) versus **4c** and **4e** (0.96−1.11 μM). Interestingly, similar structure−activity relationships among inhibitory chromone derivatives were found in drug-selected H460 lung cancer cells overexpressing ABCG2 (Table 1, right half) because (i) chromone **1** and **4a** displayed the highest potency (EC_{50} of 0.05−0.08 μM, even better than in HEK293 transfected cells) and (ii) structural modifications of the *p*-bromobenzyloxy, indole, and amide functional groups also induced alterations, with the highest effects resulting from the cumulated modifications in **4g** and **4h**.

Selectivity toward ABCG2 and Ability to Inhibit the Efflux of Other Substrate Drugs. The best inhibitory chromones in addition to **1**, as identified from Table 1 and Figure 2 (**4a**−**f**), were not able to inhibit the efflux activity of either ABCB1 or ABCC1 at 5 μM using rhodamine 123 or calcein-AM,

Scheme 3[a]

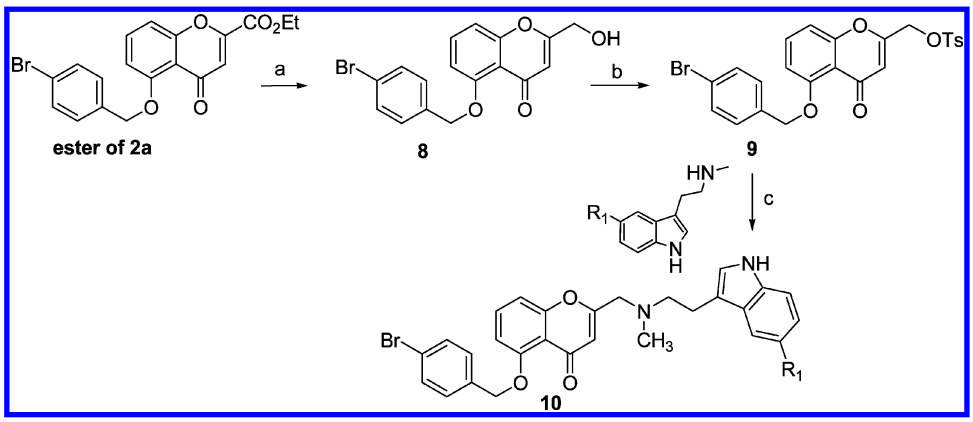

[a]Reagents and conditions: (a) $NaBH_4$, MeOH, rt; (b) TsCl, Et_3N, CH_2Cl_2, rt; (c) DMF.

dx.doi.org/10.1021/jm401649j | J. Med. Chem. 2013, 56, 9849−9860

Table 1. Efficiency of Chromone Inhibition on Mitoxantrone Efflux in Both Transfected and Drug-Selected ABCG2-Overexpressing Cancer Cells[a]

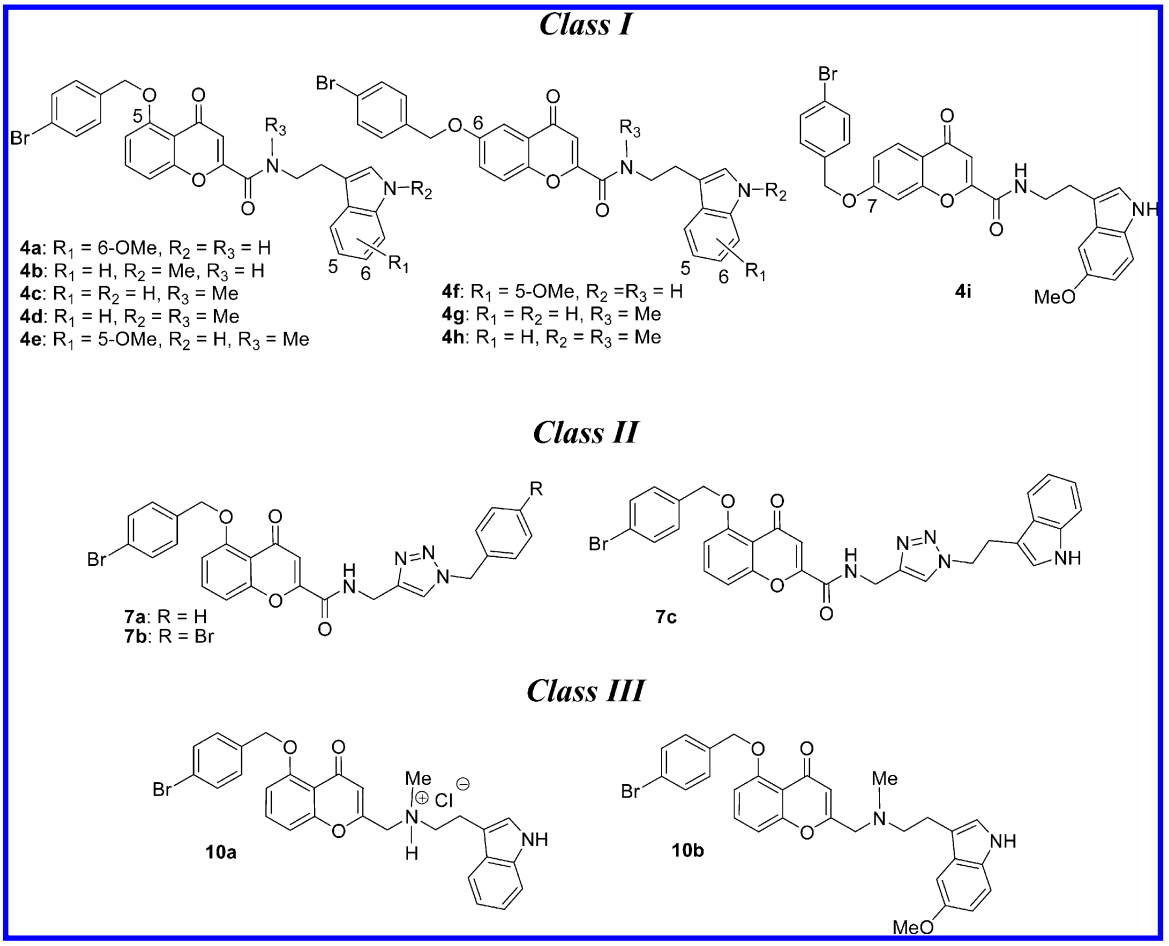

chromone	transfected HEK293 cells		drug-selected H460 cancer cells	
	EC_{50} (μM)	maximal inhibition (%)	EC_{50} (μM)	maximal inhibition (%)
Ko143	0.09 ± 0.01	106 ± 1	0.07 ± 0.01	116 ± 6
1	0.13 ± 0.09	98 ± 7	0.05 ± 0.01	107 ± 11
Class I				
4a	0.10 ± 0.03	97 ± 30	0.08 ± 0.04	89 ± 5
4b	0.30 ± 0.01	85 ± 5	0.22 ± 0.03	102 ± 8
4c	1.11 ± 0.05[b]	105 ± 29	0.57 ± 0.06[b]	89 ± 9
4d	1.00 ± 0.28	88 ± 11	0.50 ± 0.05	84 ± 12[b]
4e	0.96 ± 0.03	101 ± 20	0.53 ± 0.16	96 ± 4
4f	0.29 ± 0.14	108 ± 27	0.10 ± 0.02	109 ± 9
4g	2.58 ± 0.57[d]	54 ± 16[b]	1.67 ± 0.42[d]	50 ± 5[d]
4h	2.06 ± 0.51[d]	50 ± 15[b]	2.15 ± 0.50[d]	61 ± 1[d]
4i	1.27 ± 0.59[c]	80 ± 5	1.54 ± 0.20[d]	93 ± 8
Class II				
7a	1.52 ± 0.69[d]	78 ± 9	0.50 ± 0.13	76 ± 13[c]
7b	0.57 ± 0.01	95 ± 17	0.71 ± 0.04[c]	76 ± 6[c]
7c	0.49 ± 0.03	87 ± 17	0.46 ± 0.12	86 ± 3
Class III				
10a	1.77 ± 0.46[d]	46 ± 10[c]	1.11 ± 0.17[d]	104 ± 12
10b	1.13 ± 0.59[b]	75 ± 8	0.60 ± 0.17[b]	106 ± 13

[a]Mitoxantrone efflux was determined by measuring its cellular accumulation by flow cytometry relative to ABCG2-negative control cells. The chromone derivatives were added at increasing concentrations up to 5−10 μM, and EC_{50} values were calculated as the chromone concentrations producing half-maximal inhibition. Data are the mean ± SD of at least three independent experiments. Significant differences were determined using ANOVA followed by Dunnett's test comparing all compounds to chromone **1**. [b]$p < 0.05$. [c]$p < 0.01$. [d]$p < 0.001$.

respectively, as specific substrates (Figure 3). This result indicates that chromones are selective inhibitors of ABCG2, which was further confirmed using other substrates such as BODIPY-prazosin and pheophorbide A (Figure 4). A similar inhibition potency was produced for BODIPY-prazosin as compared to mitoxantrone. A slightly lower inhibition was observed

dx.doi.org/10.1021/jm401649j | J. Med. Chem. 2013, 56, 9849−9860

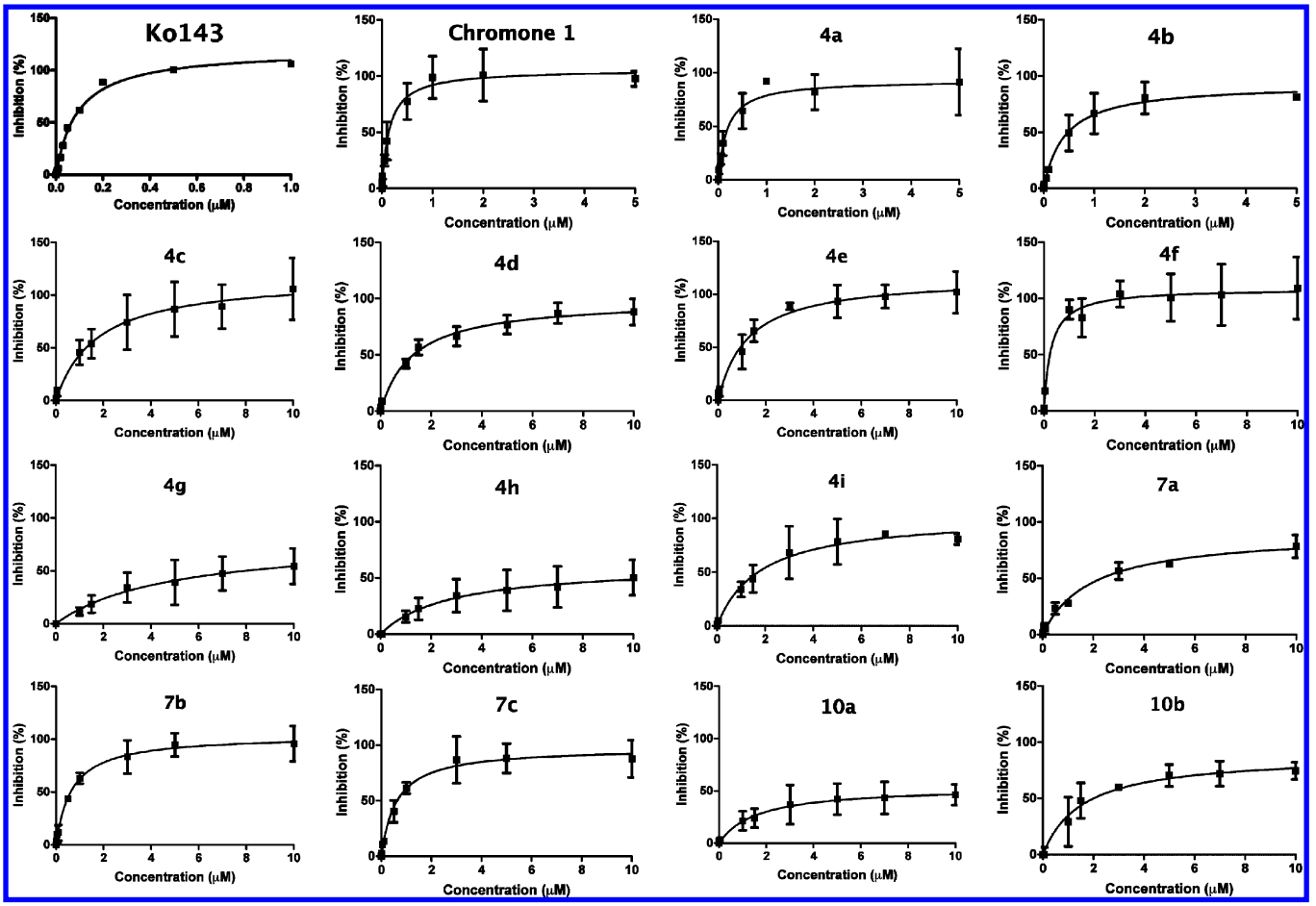

Figure 2. Concentration dependence of mitoxantrone efflux inhibition by Ko143 and the chromone derivatives in HEK293-tranfected cells. The curves with standard deviations illustrate the data from Table 1 (left half).

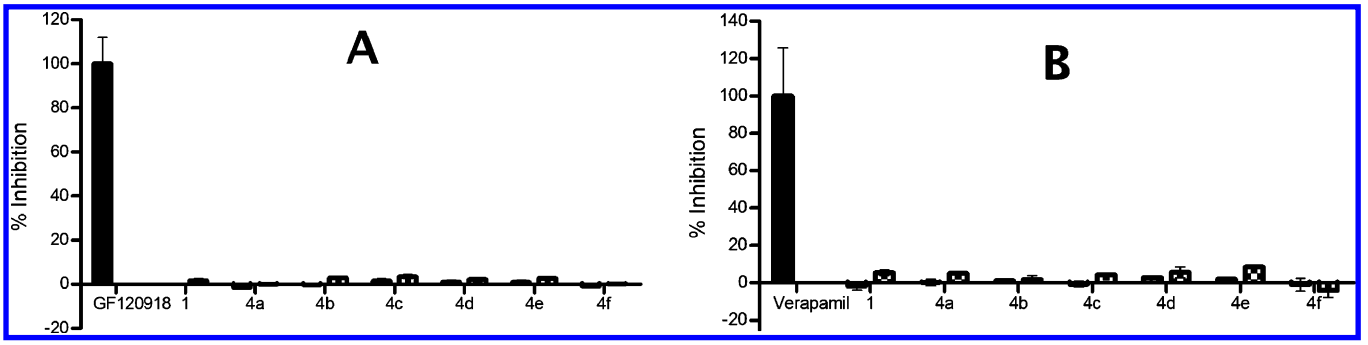

Figure 3. Inability of chromones to inhibit drug efflux mediated by either ABCB1 or ABCC1. Each chromone was assayed at 1 (left bars) and 5 μM (right bars) for its ability to alter the efflux of rhodamine 123 by ABCB1 (A) or calcein by ABCC1 (B) by flow cytometry, as was done for mitoxantrone in Table 1. The inhibition produced by the two reference inhibitors, 5 μM GF120918 and 35 μM verapamil, was taken as 100%.

for pheophorbide A, reaching a maximal value of about 80%, but the order of efficiency, **1**, **4a** > **4b**, **4f** > **4c**, **4d**, **4e**, was the same as for the two other substrates. This indicated a similar inhibition mechanism of chromones against ABCG2 drug-efflux activity regardless of drug substrates.

The inhibition produced by **4a** at a low concentration on mitoxantrone efflux from drug-selected H460 cancer cells, as shown in Table 1, was indeed able to revert multidrug resistance by chemosensitizing the cell growth to mitoxantrone toxicity in MTT assays: 0.2 μM was sufficient to produce 50% reversion of the multidrug resistance observed in untreated cells (Table 2). A lower effect was observed with **4b**, which required a 1 μM concentration to be efficient, in agreement with its 3-fold lower affinity for inhibition characterized in Table 1 (EC_{50} value of 0.22 vs 0.08 μM).

Effects on Basal and Drug-Stimulated ATPase Activities. The effects of chromone derivatives were studied on ATP hydrolysis by Sf9 insect cell membranes overexpressing human ABCG2 that were supplemented with cholesterol to produce maximal vanadate-sensitive activity. The basal ATPase activity, 8.6 ± 0.9 nmol min^{-1} mg^{-1}, was inhibited, similar to Ko143, by the first part of class I chromones (**4a**–**e**) as well as chromones from class II (**7c**) and class III (**10a** and **10b**), which all contained a *p*-bromobenzyloxy substituent at position 5,

dx.doi.org/10.1021/jm401649j | J. Med. Chem. 2013, 56, 9849–9860

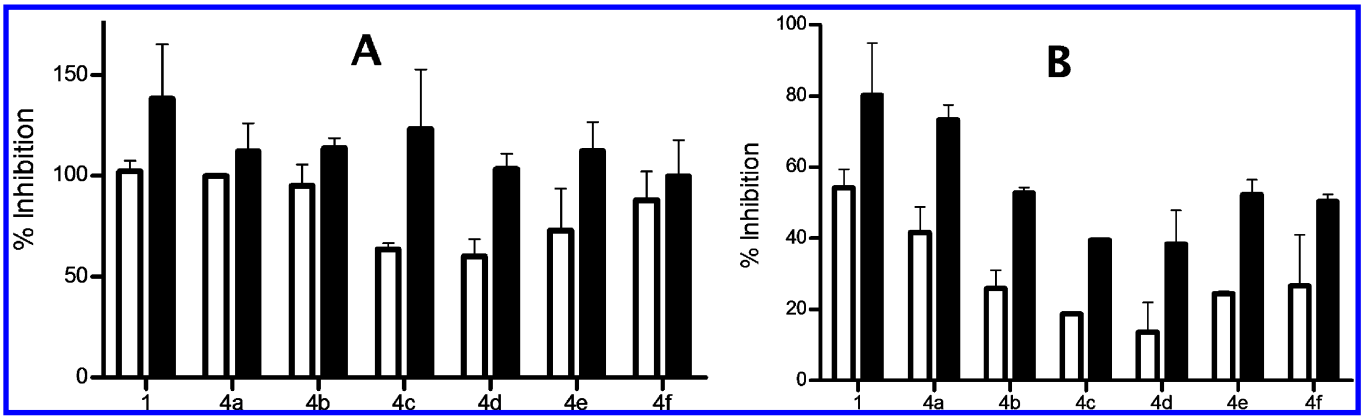

Figure 4. Inhibition by chromones of ABCG2-mediated efflux of various substrate drugs. The inhibition produced by each chromone at either 1 (white bars) or 5 μM (black bars) was studied on the efflux of BODIPY-prazosin (A) or pheophorbide A (B) by flow cytometry, as in Table 1. Data are the mean ± SD of at least three independent experiments.

Table 2. Efficiency of Chromones to Sensitize the Growth of ABCG2-Overexpressing H460 Cancer Cells to Mitoxantrone[a]

		IC_{50} (nM)			
	chromone concentration (μM)	control H460 cancer cells	drug-selected H460 cancer cells	resistance ratio	reversion of resistance (%)
no inhibitor		3.73 ± 0.79	>100	>26.8	
4a	0.2	2.13 ± 0.68	28.5 ± 4.5[b]	13.4	>50
	1.0	1.61 ± 0.14	12.1 ± 2.0[c]	7.53	>72
4b	0.2	2.87 ± 0.89	74.1 ± 20.0	25.8	>4
	1.0	1.59 ± 0.26	16.5 ± 2.3[c]	10.3	>61

[a]The viability of ABCG2-overexpressing H460 cancer cells and control H460 cells was determined upon cotreatment for 72 h with mitoxantrone (at 0−100 nM) and either chromone **4a** or **4b** at 0.2 or 1 μM. The IC_{50} values correspond to the cytotoxic mitoxantrone concentrations producing the death of 50% of cells. The percent reversion of the resistance was calculated relative to the resistance ratio of the cells not treated, with chromone inhibitor (26.8) taken as 100%. Data were collected from at least three independent experiments performed in triplicate. The Dunnett's test compared the IC_{50} values of mitoxantrone in ABCG2-overexpressing H460 cancer cells in the presence of chromones to that of mitoxantrone alone. [b]$p < 0.01$. [c]$p < 0.001$.

similar to chromone **1** (Figure 5A). Interestingly, shifting *p*-bromobenzyloxy to position 6 in **4f** induced a loss of basal ATPase inhibition, as was also observed for **4g** and **4h**. Its extended shifting to position 7 in **4i** even produced a stimulation of basal activity, 2.1-fold, similar to the transport substrates quercetin (4.1-fold), nilotinib (3.2-fold), and prazosin (2.4-fold). The (methoxy)indole was also important for basal ATPase inhibition, which was altered upon substitution by (bromo)phenyl in **7a** and **7b**, whereas modification of the linker between indole and the chromone core in **7c**, **10a**, and **10b** was not critical.

A higher, concentration-dependent inhibition was observed on the coupled or drug-stimulated ATPase activity observed in the presence of the transported substrate quercetin at 2 μM (Figure 5B). The estimated IC_{50} values indicated the following sequence in potency: (Ko143), **1**, **4a**, **7c** > **4f**, **7a** > **4b**, **7b**, **10b** > **4c**, **4d**, **4e**, **4g**, **4h**, **10a**. This confirms that N methylation of the central amine (in **10b**, **4c−e**, **4g**, **4h**, and **10a**) was highly detrimental to inhibition of coupled ATPase activity. This sequence in potency is the same as that drawn from Table 1 for inhibition of mitoxantrone efflux concerning the best (Ko143, **1**, and **4a**) and the weakest (**4c−e**, **4g**, **4h**, and **10a**) inhibitors. The single exception concerns **7a** (where both the linker and the indole were replaced).

A derivative that behaved quite differently from the others was **4i**, which inhibited drug-stimulated ATPase much more potently (IC_{50} = 0.01 μM). This might possibly be correlated to its behavior as a substrate, not an inhibitor, stimulating the basal ATPase activity (Figure 5A), although it is unknown whether this molecule is indeed transported by ABCG2.

Modulation of 5D3 Binding. Binding of the human ABCG2-specific 5D3 monoclonal antibody to an epitope located within the ECL3 extracellular loop at the surface of ABCG2-overexpressing intact cells is known to be conformation-dependent. Various conditions can modify 5D3 binding, a phenomenon called the 5D3 shift.[24] Therefore, the 5D3 binding assay provides a good tool to distinguish between transport inhibitors (such as Ko143) and transported substrates (quercetin and prazosin), the former giving a maximal 5D3 shift and the latter causing only a partial, 40−70%, increase in 5D3 binding.[25]

The ability of chromone derivatives to alter 5D3 binding is shown in Table 3. All tested chromones altered 5D3 binding, indicating that they interact with ABCG2. Moreover, the 5D3 shift assay revealed that chromones **1**, **4a−f**, **7a**, **7b**, and **10b** are potent ABCG2 inhibitors (maximal or almost maximal 5D3 shift). A low binding was observed for **4i** and **10a** at 2 μM, which might suggest transport of these chromone derivatives. In the case of **4i**, the ATPase assay also suggested the transported nature of this molecule (Figure 5A). The lowest 5D3 binding values were observed with **4h** and **4g** (40.9−47.6% at 2 μM and 72.1−79.4% at 5 μM), which correlated to the low inhibitory ability observed on both drug efflux, basal ATPase, and coupled ATPase. Therefore, these latter compounds might be potential transported substrates of ABCG2.

dx.doi.org/10.1021/jm401649j | J. Med. Chem. 2013, 56, 9849−9860

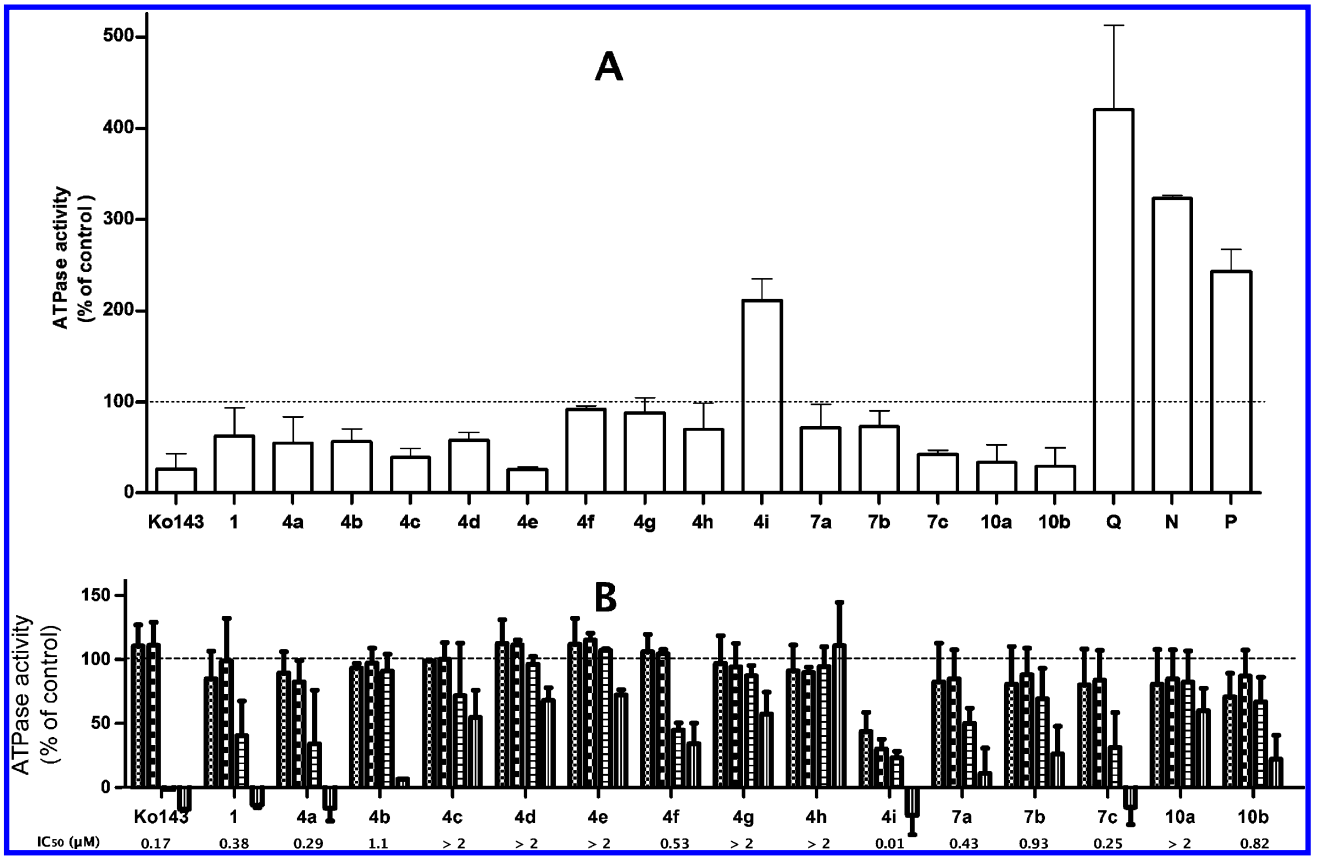

Figure 5. Effects of chromones on ABCG2 basal and substrate-stimulated ATPase activity. The effect of the compounds on vanadate-sensitive ATPase activity of wild-type ABCG2 was tested using 10 μg/sample of ABCG2-containing membrane vesicles (prepared from human ABCG2-expressing Sf9 cells loaded with cholesterol). (A) Basal ATPase activity was measured with each chromone or Ko143 at 2 μM or different transported substrates: 2 μM quercetin (Q), 0.1 μM nilotinib (N), or 20 μM prazosin (P). (B) Substrate-stimulated ATPase activity, in the presence of 2 μM quercetin, was inhibited by increasing concentrations of each chromone: 0.01, 0.03, 0.5, and 2 μM (from left to right). Data represent the mean ± SD of three independent experiments. The estimated IC_{50} values, corresponding to 50% inhibition of initial activity, are indicated under each compound.

■ DISCUSSION

The 14 new chromones evaluated in this study have allowed us to detail the mechanism of interaction of inhibitory chromones, to identify a new critical role of the central peptidic nitrogen in addition to the lateral *p*-bromobenzyloxy and (methoxy)indole substituents, and to obtain new information on the molecular mechanism of the ABCG2 target toward both drug efflux, ATPase activity, and conformational changes, as summarized in Figure 6.

Structure–Activity Relationships of Chromones as the Best ABCG2 Inhibitors. A first comparison of the different effects produced on drug-efflux activity has strengthened the important roles played by the *p*-bromobenzyloxy substituent previously identified in other chromones[13] and by the indole identified in both chalcones[26] and chromones.[13,14] The additional information obtained here concerns the effects of the *p*-bromobenzyloxy position on the basal ATPase activity, which is no longer inhibited when the substituent is shifted to position 6 and is even stimulated at position 7 (**4i**), similar to quercetin or other transport substrates.[27] The low 5D3 binding also suggests that **4i** behaves as a transport substrate of ABCG2. However, it cannot be completely excluded that **4i** might only mimic a transport substrate and then stimulate basal ATPase activity without being itself transported. The incomplete maximal inhibition produced by some derivatives, such as **4g**, **4h**, **7a**, **10b**, and especially the charged **10a** (Table 1 and Figure 2), does not appear to be due to their lower solubility in water, as was proposed for Tariquidar derivatives,[28] and is possibly due to different inhibitor binding.

A newly identified critical moiety of inhibitory chromones is the central amide linkage, which was not previously investigated, even in other series of compounds. It is found here to play a double role in inhibition: first, toward drug efflux because both affinity and the extent of maximal inhibition were altered upon N methylation, with an additional alteration upon reduction of the amide group; second, toward coupled ATPase activity, which was much less sensitive to inhibition. Both types of alterations are consistent with ABCG2 conformational changes leading to decreased 5D3 binding. It is, however, unknown if this marked deleterious effect of nitrogen methylation is due to the direct interaction with the ABCG2 binding site or to changes of the inhibitory chromones in either reactivity or structure. Chromone **1** was previously found to be among the best ABCG2 inhibitors ever reported because of its potency, selectivity, absence of transport, and especially low cytotoxicity[13] in contrast with Ko143, a highly potent inhibitor derived from neurotoxic fumitremorgin C. The high therapeutic ratio of chromone **1** makes it an excellent candidate for preclinical assays in mouse models, which is further strengthened here by the observations that, on one hand, it is at least as active in drug-selected cancer cells such as the lung H460 cell line and, on the other hand, the other derivative, **4a**, could constitute an

dx.doi.org/10.1021/jm401649j | J. Med. Chem. 2013, 56, 9849–9860

Table 3. Modulation of 5D3 Binding by the Different Chromone Derivatives[a]

chromone	5D3 binding (%) at 2 μM	5D3 binding (%) at 5 μM
1	100.5 ± 1.7	103.5 ± 3.8
4a	96.4 ± 2.6	101.0 ± 9.6
4b	88.7 ± 9.6	98.0 ± 8.0
4c	74.6 ± 14.4[c]	95.9 ± 6.1
4d	76.4 ± 5.7[b]	98.9 ± 7.5
4e	82.8 ± 2.7	97.4 ± 5.8
4f	93.3 ± 2.8	99.9 ± 6.9
4g	47.6 ± 1.9[d]	79.4 ± 0.8[d]
4h	40.9 ± 6.8[d]	72.1 ± 3.9[d]
4i	64.6 ± 11.0[d]	90.1 ± 1.5
7a	74.3 ± 6.9[c]	95.4 ± 3.8
7b	78.7 ± 14.6[b]	91.8 ± 2.5
7c	93.1 ± 8.7	105.2 ± 3.2
10a	57.4 ± 6.3[d]	95.4 ± 3.3
10b	82.3 ± 10.1	102.5 ± 2.7

[a]The binding of the ABCG2-selective 5D3 monoclonal antibody was measured by flow cytometry on *ABCG2*-transfected HEK293 cells. The fluorescence obtained with each chromone was compared with the maximal value obtained using 2 μM Ko143, which was taken as 100%. Data are the mean ± SD of at least three independent experiments. The Dunnett's test compared all chromones to Ko143. [b]$p < 0.05$. [c]$p < 0.01$. [d]$p < 0.001$.

alternative. Indeed, similar to chromone **1**, the **4a** derivative is also selective for ABCG2 over ABCB1 and ABCC1 and is able to inhibit the efflux of any drug and to sensitize the cell growth of ABCG2-overexpressing cancer cells to mitoxantrone.

New Data on ABCG2 Molecular Mechanism. Important new data about the transporter target has been brought by the present study. Indeed, basal and coupled ATPase activities appear to obey different mechanisms and/or to involve different conformations of the transporter, as was also proposed for ABCB1.[29] For ABCG2, both types of ATPase activity could be modulated separately by different modifications of the inhibitory chromones: by shifting the position of lateral *p*-bromobenzyloxy or replacing the indole for the basal ATPase activity and upon N methylation of the amide for the coupled ATPase activity. The latter, on the basis of high-resolution crystal structures available for various multidrug ABC transporters,[30−33] is recognized to allow the energy-dependent inward-facing to outward-facing conformational change required for drug translocation. The good correlation between inhibition of drug efflux and inhibition of quercetin-coupled ATPase, as evidenced by chromones, suggests a strict coupling between ATP-hydrolysis-driven energy and transmembrane substrate drug translocation through ABCG2. By contrast, very little is known about the meaning and mechanism of basal ATPase activity, which remains a matter of debate, especially because it is highly variable among ABC transporters and among species; it might be possibly involved in protein flexibility, contributing to its polyspecificity toward a wide range of substrates.

EXPERIMENTAL SECTION

Chemistry. NMR spectra were recorded on a Brüker AC-400 instrument (400 MHz). Chemical shifts (δ) are reported in ppm relative to Me_4Si (internal standard). Electrospray ionization ESI mass

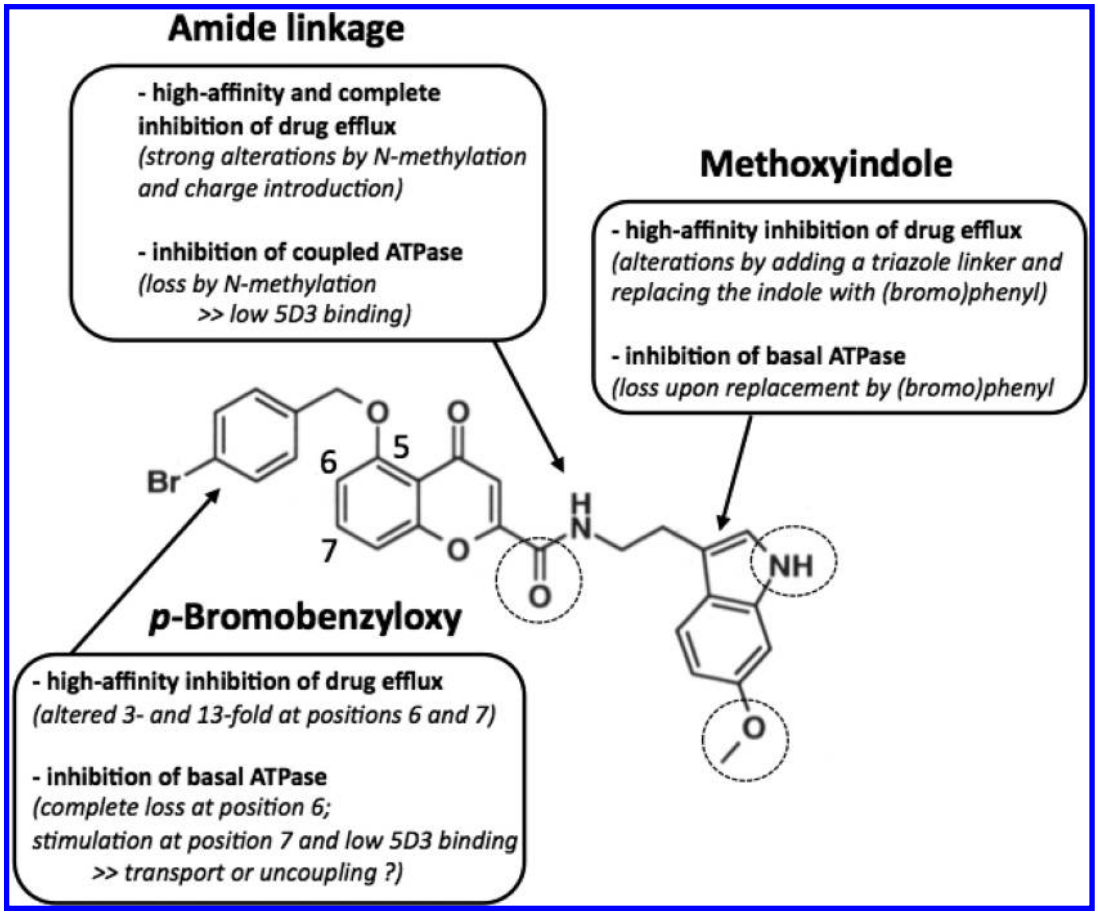

Figure 6. Schematic of the structure−activity relationships of inhibitory chromones toward drug efflux, ATPase activity, and conformational 5D3 shift.

dx.doi.org/10.1021/jm401649j | J. Med. Chem. 2013, 56, 9849−9860

spectra were acquired by the Analytical Department of Grenoble University on an Esquire 300 Plus Bruker Daltonis instrument with a nanospray inlet. Combustion analyses were performed at the Analytical Department of Grenoble University, and all tested compounds have a purity of at least 95%. Thin-layer chromatography (TLC) used Macherey-Nagel silica gel F-254 plates (thickness 0.25 mm). Flash chromatography used Merck silica gel 60, 200−400 mesh. Unless otherwise stated, reagents were obtained from commercial sources and were used without further purification.

*Synthesis of Class I Compounds (**4**).* To a solution of tryptamine derivative in dry DMF (10 mL/mmol) were added successively the carboxylic acid (1 equiv) in DMF (10 mL/mmol), HOBt (2 equiv), triethylamine (5 equiv), and EDCI (2 equiv). The mixture was stirred at room temperature for 24 h. The resulting solution was poured into 1 M HCl (15 mL) and extracted with CH_2Cl_2 (3 × 15 mL). The combined organic layers were washed with saturated $NaHCO_3$ (15 mL) and H_2O (15 mL), dried over $MgSO_4$, concentrated under reduced pressure, and suspended in diethyl ether to afford compounds **4** as white solids.

*5-(4-Bromobenzyloxy)-4-oxo-4H-chromene-2-carboxylic Acid [2-(6-Methoxy-1H-indol-3-yl)-ethyl]-amide (**4a**).* Compound **4a** was purified by column chromatography, eluting with a CH_2Cl_2/EtOAc (9:1 to 8:2) gradient. Yield 11%. mp 190−193 °C. ^{1}H NMR (400 MHz, DMSO): δ 2.93 (t, 2H, J = 7.7 Hz), 3.55 (q, 2H, J = 6.5 Hz), 3.74 (s, 3H), 5.24 (s, 2H), 6.64 (dd, 1H, J = 2.3 Hz, 8.6 Hz), 6.66 (s, 1H), 6.84 (d, 1H, J = 2.2 Hz), 7.05 (d, 1H, J = 2.2 Hz), 7.10 (d, 1H, J = 8.0 Hz), 7.25 (d, 1H, J = 8.4 Hz), 7.45 (d, 1H, J = 8.6 Hz), 7.58−7.63 (m, 4H), 7.76 (t, 1H, J = 8.4 Hz), 9.17 (t, 1H, J = 5.7 Hz), 10.62 (s, 1H). ^{13}C NMR (100 MHz, DMSO): δ 24.9, 55.1, 69.2, 94.5, 108.5, 108.9, 110.5, 111.4, 112.0, 114.5, 118.8, 120.6, 121.2, 121.6, 128.9, 131.2, 134.9, 136.3, 136.9, 153.6, 155.5, 157.0, 157.7, 158.8, 176.5. MS (ESI) m/z 545 $[M - H]^-$, 581 $[M + Cl]^-$. Anal. Calcd for $C_{28}H_{23}BrN_2O_5$: C, 61.44; H, 4.24; N, 5.12. Found: C, 61.05; H, 4.24; N, 4.91.

*5-(4-Bromobenzyloxy)-4-oxo-4H-chromene-2-carboxylic Acid [2-(1-Methyl-1H-indol-3-yl)-ethyl]-amide (**4b**).* Compound **4b** was purified by column chromatography, eluting with a CH_2Cl_2/EtOAc (95:5 to 9:1) gradient. Yield 19%. mp 177−180 °C. ^{1}H NMR (400 MHz, DMSO): δ 2.99 (t, 2H, J = 7.6 Hz), 3.57 (q, 2H, J = 7.0 Hz), 3.75 (s, 3H), 5.26 (s, 2H), 6.69 (s, 1H), 7.03 (t, 1H, J = 7.3 Hz), 7.12−7.17 (m, 2H), 7.22 (s, 1H), 7.27 (d, 1H, J = 8.4 Hz), 7.40 (d, 1H, J = 8.4 Hz), 7.60−7.66 (m, 5H), 7.79 (t, 1H, J = 8.4 Hz), 9.24 (t, 1H, J = 5.7 Hz). ^{13}C NMR (100 MHz, DMSO): δ 24.6, 32.1, 69.1, 108.8, 109.5, 110.5, 110.7, 112.0, 114.4, 118.2, 118.3, 120.5, 121.0, 127.1, 127.4, 128.8, 131.1, 134.8, 136.2, 136.5, 153.5, 156.9, 157.6, 158.8, 176.4. MS (ESI) m/z 553 $[M + Na]^+$. Anal. Calcd for $C_{28}H_{23}BrN_2O_4 \cdot {}^6/_7 H_2O$: C, 61.50; H, 4.55; N, 5.12 . Found: C, 61.49; H, 4.40; N, 5.13 .

*5-(4-Bromobenzyloxy)-4-oxo-4H-chromene-2-carboxylic Acid [2-(1H-Indol-3-yl)-ethyl]-methyl-amide (**4c**).* Compound **4c** was purified by column chromatography, eluting with a CH_2Cl_2/MeOH (99:1 to 98:2). 6:4 mixture of rotamers. Yield 32%. mp 148−151 °C. ^{1}H NMR (400 MHz, DMSO): δ 3.02 (t, 2H, J = 7.1 Hz), 3.04 (s, 1.3H), 3.06 (s, 1.7H), 3.71 (t, 2H, J = 6.7 Hz), 5.23 (s, 1.2H), 5.25 (s, 0.8H), 6.05 (s, 0.6H), 6.31 (s, 0.4H), 6.60−7.76 (m, 12H), 10.81 (s, 0.6H), 10.87 (s, 0.4H). ^{13}C NMR (100 MHz, DMSO): δ 15.1, 22.2, 23.8, 32.9, 36.4, 48.1, 50.9, 64.9, 69.3, 109.0, 109.1, 110.1, 110.3, 110.4, 110.9, 111.3, 111.4, 111.7, 112.0, 114.3, 114.6, 117.5, 118.0, 118.2, 118.3, 120.6, 120.8, 121.0, 123.0, 123.5, 126.6, 127.2, 128.9, 121.2, 134.4, 134.4, 134.7, 136.1, 136.2, 136.3, 136.4, 155.8, 156.2, 156.9, 157.2, 157.6, 157.7, 162.2, 161.6, 175.4, 175.8. MS (ESI) m/z 533 $[M + H]^+$. Anal. Calcd for $C_{28}H_{23}BrN_2O_4$: C, 63.29; H, 4.36; N, 5.27. Found: C, 63.45; H, 4.50; N, 5.22.

*5-(4-Bromobenzyloxy)-4-oxo-4H-chromene-2-carboxylic Acid [2-(1-Methyl-1H-indol-3-yl)-ethyl]-methyl-amide (**4d**).* Compound **4d** was purified by column chromatography, eluting with a CH_2Cl_2/MeOH (99:1 to 98:2) gradient. 6:4 mixture of rotamers. Yield 20%. mp 150−153 °C. ^{1}H NMR (400 MHz, DMSO): δ 2.97−3.04 (m, 2H), 3.09 (s, 3H), 3.68−3.77 (m, 5H), 5.23 (s, 1.2H), 5.25 (s, 0.8H), 5.95 (s, 0.6H), 6.32 (s 0.4H), 6.64−7.76 (m, 12H). ^{13}C NMR (100 MHz, DMSO): δ 22.0, 23.5, 32.1, 32.2, 32.9, 36.3, 48.1, 51.0, 69.2, 109.0, 109.4, 109.5, 110.2, 110.3, 111.8, 112.0, 114.2, 114.5, 117.7, 118.1, 118.4, 120.5, 120.9, 121.1, 126.9, 127.4, 127.4, 127.7, 128.9, 131.2, 134.3, 134.7, 136.3, 136.4, 136.6, 155.7, 156.1, 156.8, 157.2, 157.5, 157.6, 161.2, 161.4, 175.3, 175.8. MS (ESI) m/z 547 $[M + H]^+$. Anal. Calcd for $C_{29}H_{25}BrN_2O_4$: C, 63.86; H, 4.62; N, 5.14. Found: C, 63.52; H, 4.47; N, 5.37.

*5-(4-Bromobenzyloxy)-4-oxo-4H-chromene-2-carboxylic Acid [2-(5-Methoxy-1H-indol-3-yl)-ethyl]-methyl-amide (**4e**).* Compound **4e** was purified by column chromatography, eluting with a CH_2Cl_2/MeOH (99:1 to 98:2) gradient. 2:1 mixture of rotamers . Yield 29%. mp 168−171 °C. ^{1}H NMR (400 MHz, DMSO): δ 2.95−3.00 (m, 2H), 3.04 (s, 1.1H), 3.06 (s, 1.9H), 3.43 (s, 2H), 3.69−3.75 (m, 2H), 3.77 (s, 1H), 5.21 (s, 1.2H), 5.25 (s, 0.8H), 5.67 (s, 0.7H), 6.31 (s, 0.3H), 6.44−7.77 (m, 12H), 10.65 (s, 0.7H), 10.70 (s, 0.3H). ^{13}C NMR (100 MHz, DMSO): δ 22.2, 23.6, 32.9, 36.4, 47.9, 50.6, 54.8, 55.3, 69.2, 99.0, 100.2, 108.9, 109.1, 109.7, 110.2, 110.3, 110.6, 111.0, 111.04, 111.7, 112.0, 114.1, 120.5, 123.5, 124.2, 126.8, 127.5, 128.8, 131.1, 131.14, 131.2, 131.3, 134.3, 134.6, 136.3, 136.4, 152.8, 153.0, 155.5, 156.2, 156.7, 157.2, 157.5, 157.6, 161.1, 161.5, 175.3, 175.7. MS (ESI) m/z 563 $[M + H]^+$. Anal. Calcd for $C_{29}H_{25}BrN_2O_5$: C, 62.04; H, 4.49; N, 4.99. Found: C, 61.82; H, 4.55; N, 5.10.

*6-(4-Bromobenzyloxy)-4-oxo-4H-chromene-2-carboxylic Acid [2-(5-Methoxy-1H-indol-3-yl)-ethyl]-amide (**4f**).* Yield 41%. mp 192−194 °C. ^{1}H NMR (400 MHz, DMSO): δ 2.96 (t, 2H, J = 7.6 Hz), 3.59 (q, 2H, J = 7.2 Hz), 3.73 (s, 3H), 5.23 (s, 2H), 6.72 (dd, 1H, J = 2.4 Hz, 8.8 Hz), 6.81 (s, 1H), 7.08 (d, 1H, J = 2.3 Hz), 7.17 (d, 1H, J = 2.2 Hz), 7.23 (d, 1H, J = 8.8 Hz), 7.46 (d, 2H, J = 8.4 Hz), 7.51 (d, 1H, J = 3.2 Hz), 7.58 (dd, 1H, J = 3.2, 9.2 Hz), 7.62 (d, 2H, J = 8.4 Hz), 7.69 (d, 1H, J = 9.2 Hz), 9.24 (t, 1H, J = 5.6 Hz), 10.69 (s, 1H). ^{13}C NMR (100 MHz, DMSO): δ 24.9, 55.3, 69.1, 100.2, 106.0, 109.5, 111.0, 111.2, 112.0, 120.4, 121.1, 123.4, 124.4, 124.7, 127.5, 129.8, 129.9, 131.4, 135.9, 149.9, 153.0, 155.6, 155.8, 158.9, 176.9, 177.0. MS (ESI) m/z 546 $[M - 1]^+$. Anal. Calcd for $C_{28}H_{23}BrN_2O_5$: C, 61.44; H, 4.24; N, 5.12. Found: C, 60.91; H, 4.22; N, 4.89.

*6-(4-Bromobenzyloxy)-4-oxo-4H-chromene-2-carboxylic Acid [2-(1H-Indol-3-yl)-ethyl]-methyl-amide (**4g**).* Yield 42%. mp 179−180 °C. 6:4 mixture of rotamers. ^{1}H NMR (400 MHz, DMSO): δ 2.97−3.06 (m, 5H), 3.64−3.71 (m, 2H), 5.22 (s, 1.2H), 5.23 (0.8H), 6.16 (s, 0.6H), 6.46 (s, 0.4H), 6.50−7.68 (m, 12H), 10.80 (s, 0.6H), 10.87 (s, 0.4H). ^{13}C NMR (100 MHz, DMSO): δ 22.2, 23.7, 30.7, 32.8, 36.4, 48.1, 50.9, 68.9, 69.0, 106.1, 106.2, 109.2, 109.5, 110.0, 110.9, 111.3, 111.4, 117.4, 118.0, 118.2, 118.3, 120.2, 120.3, 120.8, 120.9, 121.0, 123.0, 123.5, 124.0, 124.3, 124.4, 126.6, 127.2, 129.8, 129.9, 131.4, 136.0, 136.1, 126.2, 149.8, 150.2, 155.5, 155.7, 157.9, 158.3, 161.3, 161.7, 175.9, 176.3, 206.5. MS (ESI) m/z 532 $[M + H]^+$, 553 $[M + Na]^+$. Anal. Calcd for $C_{28}H_{23}BrN_2O_4$: C, 63.29; H, 4.36; N, 5.27. Found: C, 62.34; H, 4.87; N, 5.24.

*6-(4-Bromobenzyloxy)-4-oxo-4H-chromene-2-carboxylic Acid [2-(Methyl-1H-indol-3-yl)-ethyl]-methyl-amide (**4h**).* Yield 3%. mp 127−131 °C. 3:2 mixture of rotamers. ^{1}H NMR (400 MHz, DMSO): δ 2.95−3.10 (m, 2H), 3.05 (s, 1.2H), 3.08 (1.8H), 3.65 (s, 1.8H), 3.66−3.70 (m, 2H), 3.75 (s, 1.2H), 5.22 (s, 1.4), 5.23 (s, 0.6H), 6.03 (s, 0.7H), 6.47 (s, 0.3H), 6.86−7.70 (m, 12H). ^{13}C NMR (100 MHz, DMSO): δ 22.1, 23.4, 32.1, 32.2, 32.6, 36.4, 48.1, 51.0, 68.9, 106.1, 109.3, 109.4, 109.5, 109.6, 110.2, 117.7, 118.1, 118.4, 120.1, 120.3, 120.6, 121.0, 121.1, 123.9, 124.0, 124.3, 126.9, 127.4, 127.8, 129.7, 131.4, 136.0, 136.1, 136.4, 136.6, 149.7, 150.2, 155.5, 155.7, 157.8, 158.3, 161.3, 161.6, 175.8, 176.3. MS (ESI) m/z 545 $[M + H]^+$, 567 $[M + Na]^+$, 1111 $[2M + Na]^+$. Anal. Calcd for $C_{29}H_{25}BrN_2O_4$: C, 63.86; H, 4.62; N, 5.14. Found: C, 63.60; H, 4.67; N, 5.37.

*7-(4-Bromobenzyloxy)-4-oxo-4H-chromene-2-carboxylic Acid [2-(5-Methoxy-1H-indol-3-yl)-ethyl]-amide (**4i**).* Yield 45%. mp 227−229 °C. ^{1}H NMR (400 MHz, DMSO): δ 2.95 (t, 2H, J = 7.6 Hz), 3.58 (q, 2H, J = 6.8 Hz), 3.74 (s, 3H), 5.27 (s, 2H), 6.71 (dd, 1H, J = 2.0 Hz, 8.4 Hz), 6.77 (s, 1H), 7.07 (d, 1H, J = 2.0 Hz), 7.16−7.24 (m, 4H), 7.45 (d, 2H, J = 8.0 Hz), 7.63 (d, 2H, J = 8.4 Hz), 7.97 (d, 1H, J = 8.8 Hz), 9.17 (t, 1H, J = 5.2 Hz), 10.68 (s, 1H). ^{13}C NMR (100 MHz, DMSO): δ 24.9, 55.3, 69.2, 100.1, 101.9, 110.5, 111.1, 111.2, 112.1, 115.7, 117.8, 121.3, 123.4, 126.5, 127.5, 129.9, 131.4, 131.5, 135.4, 153.0, 155.5, 156.8, 158.9, 163.1, 176.4. MS (ESI) m/z 531 $[M - 15]^+$. Anal. Calcd

for $C_{28}H_{23}BrN_2O_5$: C, 61.44; H, 4.24; N, 5.12. Found: C, 61.68; H, 4.13; N, 5.26.

*5-(4-Bromo-benzyloxy)-4-oxo-4H-chromene-2-carboxylic Acid Prop-2-ynylamide (**5**).* To a solution of propargylamine in dry DMF (10 mL/mmol) were added successively the carboxylic acid **2a** (1 equiv) in DMF (10 mL/mmol), HOBt (2 equiv), triethylamine (5 equiv), and EDC (2 equiv). The resulting mixture was stirred at room temperature for 24 h. The solution was poured into 1 M HCl and extracted with CH_2Cl_2. The organic layer was washed with saturated $NaHCO_3$ and H_2O, dried over $MgSO_4$, concentrated, and suspended in diethyl ether to afford the compound (**5**) as a white solid. Yield 44%. mp 234−236 °C. ^{1}H NMR (400 MHz, DMSO): δ 3.20 (t, 1H, J = 2.4 Hz), 4.09 (dd, 2H, J = 2.4, 5.6 Hz), 5.23 (s, 2H), 6.67 (s, 1H), 7.10 (d, 1H, J = 7.6 Hz), 7.26 (dd, 1H, J = 0.8, 8.8 Hz), 7.60 (m, 4H), 7.75 (t, 1H, J = 8.4 Hz), 9.54 (t, 1H, J = 5.6 Hz). ^{13}C (100 MHz, DMSO): δ 30.7, 69.2, 73.5, 80.3, 108.9, 110.6, 112.4, 114.5, 120.6, 128.9, 131.2, 135.1, 136.3, 153.0, 157.0, 157.7, 158.9, 176.5. MS (ESI) m/z 412 $[M + H]^+$.

*General Procedure for the Synthesis of Class II Compounds (**7**).* To a solution of acid **2a** in DMF (30 mL/mmol) were added azide (**6**) (1.2 equiv), sodium ascorbate (0.2 equiv), and $CuSO_4.5H_2O$ (0.1 equiv). The resulting mixture was stirred at room temperature for 24 h. The solution was poured into H_2O and extracted with ethyl acetate. The organic layers were separated and washed with H_2O, dried over $MgSO_4$, filtered, concentrated, and suspended in diethyl ether to give the desired compounds as white solids.

*5-(4-Bromo-benzyloxy)-4-oxo-4H-chromene-2-carboxylic Acid (1-Benzyl-1H [1,2,3]triazol-4-ylmethyl)-amide (**7a**).* Compound **7a** was synthesized from **2a** and benzyl azide. Yield 46%. mp 202−205 °C. ^{1}H NMR (400 MHz, DMSO): δ 4.69 (d, 2H, J = 5.2 Hz), 5.16 (s, 2H), 5.50 (s, 2H), 6.82 (d, 1H, J = 8.4 Hz), 6.98 (s, 1H), 7.02 (d, 1H, J = 8.4 Hz), 7.29 (m, 2H), 7.38 (m, 3H), 7.50 (m, 4H), 7.56 (m, 1H), 7.66, (s, 1H). ^{13}C (100 MHz, DMSO): δ 35.0, 54.7, 70.3, 109.0, 110.7, 114.0, 115.6, 121.8, 128.38, 128.4, 129.2, 129.4, 131.8, 134.2, 134.6, 135.4, 152.6, 157.4, 158.6, 159.5, 177.6. MS (ESI) m/z 567 $[M + Na]^+$. Anal. Calcd for $C_{27}H_{21}BrN_4O_4$: C, 59.46; H, 3.88; N, 10.27. Found: C, 59.00; H, 3.91; N, 10.43.

*5-(4-Bromo-benzyloxy)-4-oxo-4H-chromene-2-carboxylic Acid [1-(4-Bromobenzyl)-1H-[1,2,3]triazol-4-ylmethyl]-amide (**7b**).* Compound **7b** was synthesized from acid **2a** and 4-bromobenzyl azide. Yield 34%. mp 211−214 °C. ^{1}H NMR (400 MHz, DMSO): δ 4.51 (d, 2H, J = 5.6 Hz), 5.22 (s, 2H), 5.53 (s, 2H), 6.66 (s, 1H), 7.07 (d, 1H, J = 8.4 Hz), 7.22 (dd, 1H, J = 0.4, 8.4 Hz), 7.26 (m, 2H), 7.53−7.61 (m, 6H), 7.73 (t, 1H, J = 8.4 Hz), 8.08 (s, 1H), 9.60 (t, 1H, J = 6 Hz). ^{13}C (100 MHz, DMSO): δ 34.7, 52.0, 69.2, 108.9, 110.6, 112.3, 114.5, 120.6, 121.4, 123.4, 128.9, 130.2, 131.2, 131.6, 135.0, 135.4, 136.3, 153.3, 157.0, 157.7, 159.0, 176.5. MS (ESI) m/z 647 $[M + Na]^+$. Anal. Calcd for $C_{27}H_{20}Br_2N_4O_4$: C, 51.95; H, 3.23; N, 8.97. Found: C, 51.81; H, 3.41; N, 9.89.

*5-(4-Bromo-benzyloxy)-4-oxo-4H-chromene-2-carboxylic Acid {1-[2 (1H-Indol-3-yl)-ethyl]-1H-[1,2,3]triazol- 4-ylmethyl}-amide (**7c**).* Compound **7c** was synthesized from acid **2a** and 2-(3-indolyl)-ethylazide. Yield 10%. mp 169−171 °C. ^{1}H NMR (400 MHz, DMSO): δ 3.25 (t, 2H, J = 7.6 Hz), 4.51 (d, 2H, J = 6.0 Hz), 4.60 (t, 2H, J = 7.2 Hz), 5.24 (s, 2H), 6.68 (s, 1H), 6.93−6.97 (m, 1H), 7.01−7.05 (m, 1H), 7.09−7.11 (m, 2H), 7.25 (d, 1H, J = 8.0 Hz), 7.30 (d, 1H, J = 8.0 Hz), 7.50 (d, 1H, J = 8.0 Hz), 7.57−7.63 (m, 4H), 7.75 (t, 1H, J = 8.4 Hz), 8.04 (s, 1H), 9.62 (t, 1H, J = 5.6 Hz), 10.85 (s, 1H). ^{13}C (400 MHz, DMSO): δ 25.9, 30.6, 34.7, 49.9, 69.1, 108.8, 109.9, 110.5, 111.3, 112.2, 114.4, 118.0, 118.2, 120.5, 120.9, 123.0, 123.1, 126.8, 128.8, 131.1, 134.9, 136.0, 136.2, 153.2, 156.9, 157.6, 158.9, 176.4. MS (ESI) m/z 598 $[M + H]^+$. Anal. Calcd for $C_{30}H_{24}BrN_5O_4$: C, 60.21; H, 4.04; N, 11.70. Found: C, 58.62; H, 4.32; N, 11.31.

*5-(4-Bromobenzyloxy)-2-hydroxymethyl-chromen-4-one (**8**).* To a solution of ethyl ester of acid **2a** in anhydrous methanol (25 mL/mmol) was added $NaBH_4$ (3.65 equiv). The resulting mixture was stirred at room temperature for 20 min. The solvent was removed, and the residue was added to a solution of $NaH_2PO_4{\cdot}2H_2O$ (1.1 g in 30 mL of H_2O) and extracted with $CHCl_3$. The organic layer was dried over $MgSO_4$, concentrated, and suspended in diethyl ether overnight to give alcohol **8** as a white solid. Yield 26%. mp 144−146 °C. ^{1}H NMR (400 MHz, DMSO): δ. 4.37 (dd, 2H, J = 0.8, 6.4 Hz), 5.22 (s, 2H), 5.74 (t, 1H, J = 6.4 Hz), 6.17 (s, 1H), 7.03 (dd, 1H, J = 0.4, 8.0 Hz), 7.11 (dd, 1H, J = 0.8, 8.4 Hz), 7.56−7.62 (m, 4H), 7.65 (t, 1H, J = 8.4 Hz). ^{13}C NMR (100 MHz, DMSO): δ 59.4, 69.2, 108.6, 108.9, 110.2, 114.2, 120.5, 128.9, 131.2, 134.1, 136.5, 157.6, 157.7, 166.9, 176.3. MS (ESI) m/z 359 $[M - H]^+$.

*Toluene-4-sulfonic Acid 5-(4-Bromobenzyloxy)-4-oxo-4H-chromen-2-ylmethyl ester (**9**).* To a solution of alcohol **8** and triethylamine (3.2 equiv) in CH_2Cl_2 at 0 °C was added dropwise a solution of tosyl chloride (2.25 equiv) in CH_2Cl_2. The resulting mixture was stirred for 5 h, poured into 1 M HCl, and extracted with CH_2Cl_2. The organic layers were washed with $NaHCO_3$ and H_2O, dried over $MgSO_4$, filtered, and concentrated. The residue was purified by column chromatography, eluting with a cyclohexane/acetone (9:1 to 8:2) gradient to provide **9** as a white powder. Yield 45%. mp 133−135 °C. ^{1}H NMR (400 MHz, DMSO): δ 2.35 (s, 3H), 5.14 (s, 2H), 5.23 (s, 2H), 6.27 (s, 1H), 6.95 (d, 1H, J = 8.8 Hz), 7.04 (d, 1H, J = 8.4 Hz), 7.41 (d, 2H, J = 8.4 Hz), 7.55−7.68 (m, 5H), 7.82 (d, 2H, J = 8.4 Hz).). ^{13}C NMR (100 MHz, DMSO): δ 21.0, 67.5, 69.2, 108.9, 110.1, 113.4, 120.6, 125.5, 127.9, 128.9, 130.1, 131.2, 134.6, 136.3, 145.4, 157.4, 157.5, 157.6, 176.8. MS (ESI) m/z 517 $[M + H]^+$.

*Synthesis of Class III Compounds (**10**).* A mixture of tryptamine derivative and tosylate derivative **9** was stirred in DMF (10 mL/mmol) at room temperature for 24 h. The mixture was poured into H_2O and extracted with ethyl acetate. The organic layers were washed with H_2O, dried over $MgSO_4$, filtered, and concentrated. The residue was purified by column chromatography, eluting with a cyclohexane/acetone (9:1 to 7:3) gradient to provide compounds **10**.

*5-(4-Bromobenzyloxy)-2-({[2-(1H-indol-3-yl)-ethyl]-methyl-amino}-methyl)-chromen-4-one Hydrochloride Salt (**10a**).* Compound **10a** was synthesized from *N*-methyltryptamine and tosylate **9**. White solid. The free base was obtained after purification on column chromatography. Yield 31%. The hydrochloride salt was formed by adding hydrochloric acid in ether to a solution of free base in dry ethanol. Evaporation of ethanol following by precipitation in ether afforded **10a**. mp 159 °C. ^{1}H NMR (400 MHz, DMSO): δ 2.38 (s, 3H), 2.72−2.77 (m, 2H), 2.87−2.91 (m, 2H), 3.58 (s, 2H), 5.22 (s, 2H), 6.20 (s, 1H), 6.92 (t, 1H, J = 8.0 Hz), 7.02−7.05 (m, 2H), 7.11 (d, 1H, J = 8.0 Hz), 7.16 (d, 1H, J = 2.0 Hz), 7.31 (d, 1H, J = 8.0 Hz), 7.48 (d, 1H, J = 7.6 Hz), 7.57−7.66 (m, 5H), 10.81 (s, 1H). ^{13}C NMR (100 MHz, DMSO): δ 15.2, 19.8, 19.9, 54.7, 55.6, 64.9, 69.3, 108.9, 110.4, 111.6, 114.2, 118.3, 118.5, 120.6, 121.2, 123.3, 126.7, 128.9, 131.2, 134.6, 136.4, 136.3, 157.6, 157.7, 175.1, 175.9. MS (ESI) m/z 517 $[M + H]^+$. Anal. Calcd for $C_{28}H_{26}BrClN_2O_3{\cdot}2H_2O$: C, 57.01; H, 5.12; N, 4.75. Found: C, 57.33; H, 5.11 ; N, 4.52 .

*5-(4-Bromobenzyloxy)-2-({[2-(5-methoxy-1H-indole-3-yl)-ethyl]-methyl-amino}-methyl)-chromen-4-one (**10b**).* Compound **10b** was synthesized from 5-methoxy-*Nb*-methyltryptamine and tosylate **9**. White solid. Yield 38%. mp 64−67 °C. ^{1}H NMR (400 MHz, DMSO): δ 2.39 (s, 3H), 2.66−2.75 (m, 2H), 2.84−2.88 (m, 2H), 3.58 (s, 2H), 3.68 (s, 3H), 5.22 (s, 2H), 6.22 (s, 1H), 6.67 (dd, 1H, J = 2.4, 8.8 Hz), 6.93 (d, 1H, J = 2 Hz), 7.03 (d, 1H, J = 8.4 Hz), 7.10−7.12 (m, 2H), 7.19 (d, 1H, J = 8.8 Hz), 7.57−7.60 (m, 4H), 7.64 (t, 1H, J = 8.4 Hz), 10.60 (s, 1H). ^{13}C NMR (100 MHz, DMSO): δ 22.8, 26.3, 29.6, 55.2, 57.4, 57.8, 69.2, 99.9, 108.6, 110.3, 110.9, 111.7, 111.9, 114.2, 120.5, 123.2, 127.5, 128.9, 131.2, 131.3, 134.1, 136.5, 152.9, 157.7, 157.8, 164.5, 176.2. MS (ESI) m/z 545 $[M - H]^+$. Anal. Calcd for $C_{29}H_{27}BrN_2O_4$: C, 63.63; H, 4.97; N, 5.12. Found: C, 63.81; H, 5.00; N, 5.23.

Biology and Biochemistry. *Compounds.* Mitoxantrone, quercetin, Ko143, ouabain, DTT, EGTA, ATP, and sodium orthovanadate were purchased from Sigma-Aldrich (France). Anti-human ABCG2 (5D3 clone) and anti-mouse IgG2b K isotype control were purchased from eBioscience. Alexa Fluor 488 goat anti-mouse IgG was purchased from Life Technologies. All other reagents were commercial products of the highest available purity grade.

Cell Culture. The HEK293 human fibroblast cell line transfected with ABCG2 (HEK293-*ABCG2*) or the empty vector (HEK293-pcDNA3.1) were obtained as previously described.[13] The wild-type human lung cancer H460 cell line and the H460 mitoxantrone-selected

cells were kindly provided by Drs. R.W. Robey and SE. Bates (NCI, Bethesda, MD). The HEK293 cells and H460 cells were maintained in Dulbecco's modified Eagle's medium (DMEM high glucose) and RPMI-1640, respectively, supplemented with 10% fetal bovine serum (FBS) and 1% penicillin/streptomycin and in some cases with 0.75 mg/mL of G418 (HEK293-pcDNA3.1 and HEK293-*ABCG2*) or 20 nM mitoxantrone (H460-selected).

Inhibition of ABCG2-Mediated Drug Efflux. Cells were seeded at a density of 1.5×10^5 cells/well into 24-well culture plates. After 48 h of incubation, the cells were exposed to mitoxantrone (5 μM), BODIPY-prazosin (0.2 μM), or pheophorbide A (2 μM) for 30 min at 37 °C in the presence or absence of compounds at various concentrations and were then washed with phosphate buffered saline (PBS) and trypsinized. The intracellular fluorescence was monitored with a FACS Calibur cytometer (Becton Dickinson) using the FL4 channel, and at least 10 000 events were collected. The percentage of inhibition was calculated using the following equation: percent inhibition = $(C - M)/(C_{ev} - M) \times 100$, where C corresponds to the intracellular fluorescence of resistant cells (HEK293-*ABCG2* or drug-selected H460) in the presence of compounds and mitoxantrone, M corresponds to the intracellular fluorescence of resistant cells in the presence of only mitoxantrone, and C_{ev} corresponds to the intracellular fluorescence of control cells (HEK293-pcDNA3.1 or wild-type H460) in the presence of compounds and mitoxantrone. The EC_{50} values corresponding to concentrations producing half-maximal inhibition were calculated using nonlinear curve fitting (GraphPad Prism5) and a one-site binding hyperbola.

Effects on ABCB1- and ABCC1-Mediated Drug Efflux. NIH-3T3 cells transfected with *ABCB1* were cultured in DMEM with 60 nM colchicine/mL and seeded at a density of 6×10^4 cells/well into 24-well culture plates and incubated for 48 h at 37 °C in 5% CO_2, whereas HEK293 cells transfected with *ABCC1* were cultured with 200 μg hygromycin/mL and seeded at 2.5×10^5 cells/well for 72 h. The cells were respectively exposed to rhodamine 123 (0.5 μM) or calcein-AM (0.2 μM) for 30 min at 37 °C in the presence or absence of chromones at 1 or 5 μM, then washed with phosphate buffered saline (PBS), and trypsinized. The intracellular fluorescence was monitored with a FACS Calibur cytometer (Becton Dickinson) using the FL1 channel, and at least 10 000 events were collected. The percentage of inhibition was calculated relatively to 5 μM GF120918 or 35 μM verapamil, respectively, producing complete inhibition.

ATPase Activity Assay. Vanadate-sensitive ATPase activity was measured colorimetrically by determining the liberation of inorganic phosphate from ATP.[27] The Sf9 membranes were prepared as previously[24] and loaded with 2 mM cholesterol-RAMEB (Cyclolab Hungary).[34] The incubation was performed in 96-well plates. Sf9 membranes (0.5 mg/mL) were incubated in a 50 mM Tris-HCl and 50 mM NaCl buffer (pH 8.0) containing sodium azide (3.3 mM), ouabain (1 mM), DTT (2 mM), EGTA (0.4 mM), and the tested compounds (2 μM) with or without sodium orthovanadate (0.33 mM). The reaction was started by the addition of ATP-Mg (3.9 mM), and the plates were incubated for 30 min at 37 °C. The reaction was stopped with sodium dodecylsulfate (10%) and revealed with a mixture of ammonium molybdate reagent and 10% ascorbic acid (1:4). The absorbance was measured at 880 nm using a reader plate after a 30 min incubation.

5D3 Shift Assay.[25] Aliquots of HEK293-*ABCG2*-transfected cells (0.5×10^6 cells/tube) were centrifuged at 200*g* for 5 min at 37 °C. The pellet was washed and suspended in PBS containing 0.5% BSA. Aliquots of the suspension were incubated with tested compounds at 2 or 5 μM and with the 5D3 primary antibody (purified antihuman *ABCG2*, 5D3 clone) or the isotype control (1 μg/mL) for 45 min at 37 °C. After washing, the cells were labeled by anti-mouse Alexa Fluor 488 secondary antibody (3 μg/mL) for 30 min at 37 °C. After washing, the cells were resuspended in PBS (0.5% BSA), and 5D3 binding was determined by flow cytometry. The relative level of 5D3 binding was calculated in comparison with the fluorescence measured in the presence of Ko143, which was taken as 100% of 5D3 binding.

Mitoxantrone-Induced Cytotoxicity and Chemosensitization by Chromones. Cell survival was studied using MTT colorimetric assay.[35] Control H460 cells and ABCG2-overexpressing H460 selected cells were seeded at a density of 1×10^3 cells/well and 3×10^3 cells/well, respectively, into 96-well culture plates and incubated for 24 h at 37 °C in 5% CO_2. The cells were treated with mitoxantrone (0–100 nM) in the presence or absence of chromones **4a** and **4b** at 1 and 5 μM for 72 h. Then, 20 μL of MTT solution (5 mg/mL) was added to each well, and the plates were incubated for 4 h at 37 °C. The culture medium was discarded, and 100 μL of a solution of DMSO/ethanol (1:1) was added into each well and mixed by gently shaking for 10 min. Absorbance was measured in a microplate reader at 570 nm, and the value measured at 690 nm was subtracted. Data are the mean ± SD of at least three independent experiments.

AUTHOR INFORMATION

Corresponding Author

*E-mail: a.dipietro@ibcp.fr; Phone (+33) 47272 2629; Fax (+33) 47272 2604.

Author Contributions

▽Both junior investigators equally contributed to the work.

Author Contributions

○Both senior investigators equally contributed to the work.

Notes

The authors declare no competing financial interest.

ACKNOWLEDGMENTS

Drs. R.W. Robey and S.E. Bates, NIH, NCI Bethesda, MD, are acknowleged for providing the mitoxantrone-selected H460 lung cancer cell line together with its parental cell line. E.W. is a recipient of a mobility fellowship from the Brazilian CAPES (process no. 8792127). C.G. is a recipient of a doctoral fellowship from the Ligue Nationale Contre le Cancer. G.S. is supported by a Momentum Grant. Financial support was provided by the CNRS and Université Lyon 1 (UMR 5086), the Ligue Nationale Contre le Cancer (Equipe labellisée Ligue 2013), the Région Rhône-Alpes (CIBLE 2010), and an international grant from French ANR and Hungarian NIH (2010-INT-1101-01). A.B. is grateful to ANR Labex Arcane (ANR-11-LABX-0003-01).

ABBEVIATIONS USED

ABC, ATP-binding cassette; BCRP, breast cancer resistance protein (ABCG2); EDC, 1-ethyl-3-(3-dimethylaminopropyl)-carbodiimide; FTC, Fumitremorgin C; HOBt, hydroxybenzotriazole; MRP1, multidrug resistance protein 1 (ABCC1); P-gp, P-glycoprotein (ABCB1)

REFERENCES

(1) Endicott, J. A.; Ling, V. The biochemistry of P-glycoprotein-mediated multidrug resistance. *Annu. Rev. Biochem.* **1989**, *58*, 89–101.

(2) Cole, S. P. C.; Bhardwaj, G.; Gerlach, J. H.; Mackie, J. E.; Grant, C. E.; Almquist, K. C.; Stewart, A. J.; Kurz, E. U.; Duncan, A. M. V.; Deeley, R. G. Overexpression of a transporter gene in a multidrug-resistant human lung cancer cell line. *Science* **1993**, *258*, 1650–1654.

(3) Allikmets, R.; Schriml, L. M.; Hutchinson, A.; Romano-Spica, V.; Dean, M. A human placenta-specific ATP-binding cassette gene (ABCP) on chromosome 4q22 that is involved in multidrug resistance. *Cancer Res.* **1998**, *58*, 5337–5339.

(4) Doyle, L. A.; Yang, W.; Abruzzo, L. V.; Krogmann, T.; Gao, Y.; Rishi, A. K.; Ross, D. D. A multidrug resistance transporter from human MCF-7 breast cancer cells. *Proc. Natl. Acad. Sci. U.S.A.* **1998**, *95*, 15665–15670.

(5) Miyake, K.; Mickley, L.; Litman, T.; Zhan, Z.; Robey, R.; Cristensen, B.; Brangi, M.; Greenberger, L.; Dean, M.; Fojo, T.; Bates, S. E. Molecular cloning of cDNAs which are highly overexpressed in mitoxantrone-resistant cells: Demonstration of homology to ABC transport genes. *Cancer Res.* **1999**, *59*, 8–13.

(6) Rabindran, S. K.; He, H.; Singh, M.; Brown, E.; Collins, K. I.; Annable, T.; Greenberger, L. M. Reversal of a novel multidrug resistance mechanism in human colon carcinoma cells by fumitremorgin C. *Cancer Res.* **1998**, *58*, 5850−5858.
(7) van Loevezijn, A.; Allen, J. D.; Schinkel, A. H.; Koomen, G. J. Inhibition of BCRP-mediated drug efflux by fumitremorgin-type indolyl diketopiperazines. *Bioorg. Med. Chem. Lett.* **2001**, *11*, 29−32.
(8) Allen, J. D.; van Loevezijn, A.; Lakhai, J. M.; van der Valk, M.; van Tellingen, O.; Reid, G.; Schellens, J. H. M.; Koomen, G. J.; Schinkel, A. H. Potent and specific inhibition of the breast cancer resistance protein multidrug transporter in vitro and in mouse intestine by a novel analogue of fumitremorgin C. *Mol. Cancer Ther.* **2002**, *1*, 417−425.
(9) Boumendjel, A.; Macalou, S.; Ahmed-Belkacem, A.; Blanc, M.; Di Pietro, A. Acridone derivatives: Design, synthesis, and inhibition of breast cancer resistance protein ABCG2. *Bioorg. Med. Chem.* **2007**, *15*, 2892−2897.
(10) Kühnle, M.; Egger, M.; Muller, C.; Mahringer, A.; Bernhardt, G.; Fricker, G.; Konig, B.; Buschauer, A. Potent and selective inhibitors of breast cancer resistance protein (ABCG2) derived from the p-glycoprotein (ABCB1) modulator tariquidar. *J. Med. Chem.* **2009**, *52*, 1190−1197.
(11) Pick, A.; Müller, H.; Wiese, M. Novel lead for potent inhibitors of breast cancer resistance protein (BCRP). *Bioorg. Med. Chem. Lett.* **2010**, *20*, 180−183.
(12) Arnaud, O.; Boumendjel, A.; Gèze, A.; Honorat, M.; Matera, E. L.; Guitton, J.; Stein, W. D.; Bates, S. E.; Falson, P.; Dumontet, C.; Di Pietro, A.; Payen, L. The acridone derivative MBLI-87 sensitizes breast cancer resistance protein-expressing xenografts to irinotecan. *Eur. J. Cancer* **2011**, *47*, 640−648.
(13) Valdameri, G.; Genoux-Bastide, E.; Peres, B.; Gauthier, C.; Guitton, J.; Terreux, R.; Winnischofer, S. M.; Rocha, M. E.; Boumendjel, A.; Di Pietro, A. Substituted chromones as highly potent nontoxic inhibitors, specific for the breast cancer resistance protein. *J. Med. Chem.* **2012**, *55*, 966−970.
(14) Valdameri, G.; Genoux-Bastide, E.; Gauthier, C.; Peres, B.; Terreux, R.; Winnischofer, S. M.; Rocha, M. E.; Di Pietro, A.; Boumendjel, A. 6-Halogenochromones bearing tryptamine: One-step access to potent and highly selective inhibitors of breast cancer resistance protein. *ChemMedChem.* **2012**, *7*, 1177−1180.
(15) Hadjeri, M.; Barbier, M.; Ronot, X.; Mariotte, A.-M.; Boumendjel, A.; Boutonnat, J. Modulation of P-glycoprotein-mediated multidrug resistance by flavonoid derivatives and analogues. *J. Med. Chem.* **2003**, *46*, 2125−2131.
(16) Lynch, J. K.; Freeman, J. C.; Judd, A. S.; Iyengar, R.; Mulhern, M.; Zhao, G.; Napier, J. J.; Wodka, D.; Brodjian, S.; Dayton, B. D.; Falls, D.; Ogiela, C.; Reilly, R. M.; Campbell, T. J.; Polakowski, J. S.; Hernandez, L.; Marsh, K. C.; Shapiro, R.; Knourek-Segel, V.; Droz, B.; Bush, E.; Brune, M.; Preusser, L. C.; Fryer, R. M.; Reinhart, G. A.; Houseman, K.; Diaz, G.; Mikhail, A.; Limberis, J. T.; Sham, H. L.; Collins, C. A.; Kym, P. R. Optimization of chromone-2-carboxamide melanin concentrating hormone receptor 1 antagonists: Assessment of potency, efficacy, and cardiovascular safety. *J. Med. Chem.* **2006**, *49*, 6569−6584.
(17) Somei, M.; Yamada, F .; Kurauchi, T.; Nagahama, Y.; Hasegawa, M.; Yamada, K.; Teranishi, S.; Sato, H.; Kaneko, C. The chemistry of indoles. CIII. Simple syntheses of serotonin, *N*-methylserotonin, bufotenine, 5-methoxy-*N*-methyltryptamine, bufobutanoic acid, *N*-(indol-3-yl)methyl-5-methoxy-*N*-methyltryptamine, and lespedamine based on 1-hydroxyindole chemistry. *Chem. Pharm. Bull.* **2001**, *49*, 87−96.
(18) Pérez, E. G.; Cassels, B. K.; Eibl, C.; Gündisch, D. Synthesis and evaluation of N1-alkylindole-3-ylalkylammonium compounds as nicotinic acetylcholine receptor ligands. *Bioorg. Med. Chem.* **2012**, *20*, 3719−3727.
(19) Jenkins, P. R.; Wilson, J.; Emmerson, D.; Garcia, M. D.; Smith, M. R.; Gray, S. J.; Britton, R. G.; Mahale, S.; Chaudhuri, B. Design, synthesis and biological evaluation of new tryptamine and tetrahydro-*β*-carboline-based selective inhibitors of CDK4. *Bioorg. Med. Chem.* **2008**, *16*, 7728−7739.
(20) Song, H.; Yang, J.; Chen, W.; Qin, Y. Synthesis of chiral 3-substituted hexahydropyrroloindoline via intermolecular cyclopropanation. *Org. Lett.* **2006**, *8*, 6011−6014.
(21) Kolb, H. C.; Finn, M. G.; Sharpless, K. B. Click chemistry: Diverse chemical function from a few good reactions. *Angew. Chem., Int. Ed.* **2001**, *40*, 2004−2021.
(22) Belei, D.; Dumea, C.; Samson, A.; Farce, A.; Dubois, J.; Bîcu, E.; Ghinet, A. New farnesyltransferase inhibitors in the phenothiazine series. *Bioorg. Med. Chem. Lett.* **2012**, *22*, 4517−4522.
(23) Boumendjel, A.; Nicolle, E.; Moraux, T.; Gerby, B.; Blanc, M.; Ronot, X.; Boutonnat, J. Piperazinobenzopyranones and phenalkylaminobenzopyranones: Potent inhibitors ofbreast cancer resistance protein (ABCG2). *J. Med. Chem.* **2005**, *48*, 7275−7281.
(24) Ozvegy-Laczka, C.; Varady, G.; Koblos, G.; Uhelly, O.; Cervenak, J.; Schuetz, J. D.; Sorrentino, B. P.; Koomen, G. J.; Varadi, A.; Nemet, K.; Sarkadi, B. Function-dependent conformational changes of the ABCG2 multidrug transporter modify its interaction with a monoclonal antibody on the cell surface. *J. Biol. Chem.* **2005**, *280*, 4219−4227.
(25) Telbisz, A.; Hegedus, C.; Ozvegy-Laczka, C.; Goda, K.; Varady, G.; Takats, Z.; Szabo, E.; Sorrentino, B. P.; Varadi, A.; Sarkadi, B. Antibody binding shift assay for rapid screening of drug interactions with the human ABCG2 multidrug transporter. *Eur. J. Pharm. Sci.* **2012**, *45*, 101−109.
(26) Gauthier, C.; Valdameri, G.; Terreux, R.; Kachadourian, R.; Day, B. J.; Winnischofer, S. M.; Rocha, M. E.; Frachet, V.; Ronot, X.; Di Pietro, A.; Boumendjel, A. Investigation of chalcones as selective inhibitors of the breast cancer resistance protein ABCG2: Critical role of methoxy substituents in both inhibition and cytotoxicity. *J. Med. Chem.* **2012**, *55*, 3193−3200.
(27) Ozvegy, C.; Litman, T.; Szakacs, G.; Nagy, Z.; Bates, S. E.; Varadi, A.; Sarkadi, B. Functional characterization of the human multidrug transporter, ABCG2, expressed in insect cells. *Biochem. Biophys. Res. Commun.* **2001**, *285*, 111−117.
(28) Puentes, C. O.; Höcherl, P.; Kühnle, M.; Bauer, S.; Bürger, K.; Bernhardt, G.; Buschauer, A.; König, B. Solid phase synthesis of tariquidar-related modulators of ABC transporters preferring breast cancer resistance protein (ABCG2). *Bioorg. Med. Chem. Lett.* **2011**, *21*, 3654−3657.
(29) Al-Shawi, M. K.; Polar, M. K.; Omote, H.; Figler, R. A. Transition state analysis of the coupling of drug transport to ATP hydrolysis by P-glycoprotein. *J. Bio. Chem.* **2003**, *278*, 52629−52640.
(30) Dawson, R. J.; Locher, K. P. Structure of a bacterial multidrug ABC transporter. *Nature* **2006**, *443*, 180−185.
(31) Ward, A.; Reyes, C. L.; Yu, J.; Roth, C. B.; Chang, G. Flexibility in the ABC transporter MsbA: Alternating access with a twist. *Proc. Natl. Acad. Sci. U.S.A.* **2007**, *104*, 19005−19010.
(32) Aller, S. G.; Ward, A.; Weng, Y.; Chittaboina, S.; Zhuo, R.; Harrell, P. M.; Trinh, Y. T.; Zhang, Q.; Urbatsch, I. L.; Chang, G. Structure of P-glycoprotein reveals a molecular basis for poly-specificity drug binding. *Science* **2009**, *323*, 1718−1722.
(33) Jin, M. S.; Oldham, M. L.; Zhang, Q.; Chen, J. Crystal structure of the multidrug transporter P-glycoprotein from Caenorhabditis elegans. *Nature* **2012**, *490*, 566−569.
(34) Telbisz, A.; Muller, M.; Ozvegy-Laczka, C.; Homolya, L.; Szente, L.; Varadi, A.; Sarkadi, B. Membrane cholesterol selectively modulates the activity of the human ABCG2 multidrug transporter. *Biochim. Biophys. Acta* **2007**, *1768*, 2698−2713.
(35) Mosmann, T. Rapid colorimetric assay for cellular growth and survival: Application to proliferation and cyto-toxicity assays. *J. Immunol. Methods* **1983**, *65*, 55−63.